Chapter II.17

Physics and accelerators for particle therapy

Jacobus Maarten Schippers
Paul Scherrer Institute, Villigen, Switzerland
University Medical Center, Groningen, the Netherlands

At the Paul Scherer Institute (PSI) radiation therapy is performed by means of proton beams. Proton therapy is one of the particle therapies, in which energetic ions (mostly protons and carbon ions) are used to treat cancer patient by irradiating the tumor with high precision. At PSI the radiation dose is applied by a proton beam of max 250 MeV. In this chapter, the interactions of energetic ions with matter (tissue) and the way particle therapy is applied are discussed, followed by a description of the PSI's medical proton cyclotron and the treatment rooms in which the dose is applied to the patient.

II.17.1 Introduction: particle therapy

Already since the discovery of X-rays in 1895, ionizing radiation has been used to treat cancer with radiation therapy. However, in 1946 Robert Wilson suggested to apply proton beams for this purpose [1]. He proposed to use the high dose peak, which occurs just before the end of the proton range in tissue, to apply a high radiation dose selectively into a tumour. The first patient was treated with protons in Berkeley in 1950 [2]. To accelerate protons and ions to energies needed for particle therapy, usually cyclotrons and synchrotrons have been used since then. In the first 50 years of particle therapy, many treatment facilities were located at accelerators based in physics laboratories. The first hospital based facility for proton therapy started treatment of tumors in the eye at the cyclotron of the Clatterbridge Cancer Centre (GB) in 1989, see Ref. [3], and the first particle therapy facility for treatment of other kinds of tumours, came in operation at the Loma Linda University Medical Center (CA, USA) in 1991 [4]. In this big hospital based facility a dedicated synchrotron was coupled to three gantries. Gantries are large mechanical constructions with a typical diameter of 10^{-12} m, to support beam transport components. These gantries can thus rotate around the patient to aim the beam from different directions to the tumour. Since then commercial companies have increased interest to produce the equipment and offer complete treatment facilities, including gantries. Since the beginning of this century, the number of clinical facilities in a hospital environment has been increasing and these are currently the standard treatment facilities for proton or carbon ion therapy. In 2020 the worldwide number of facilities has increased to more than 110 [12], in which more than 300 000 patients have been treated with protons (approx. 85%) or carbon ions (approx. 15%). Other ions are applied in research programs, but only at a few places in the world. Today, the cyclotron and the synchrotron are the two typical types of accelerators offered by companies and they have proven their reliability in clinical facilities, an example of which is shown in Fig. II.17.1.

This chapter should be cited as: Physics and accelerators for particle therapy, J. M. Schippers, DOI: 10.23730/CYRSP-2024-003.1841, in: Proceedings of the Joint Universities Accelerator School (JUAS): Courses and exercises, E. Métral (ed.), CERN Yellow Reports: School Proceedings, CERN-2024-003, DOI: 10.23730/CYRSP-2024-003, p. 1841.

There are many textbooks and proceedings from accelerator schools. An example of a good overview of accelerator designs for clinical applications is given in Ref. [5].

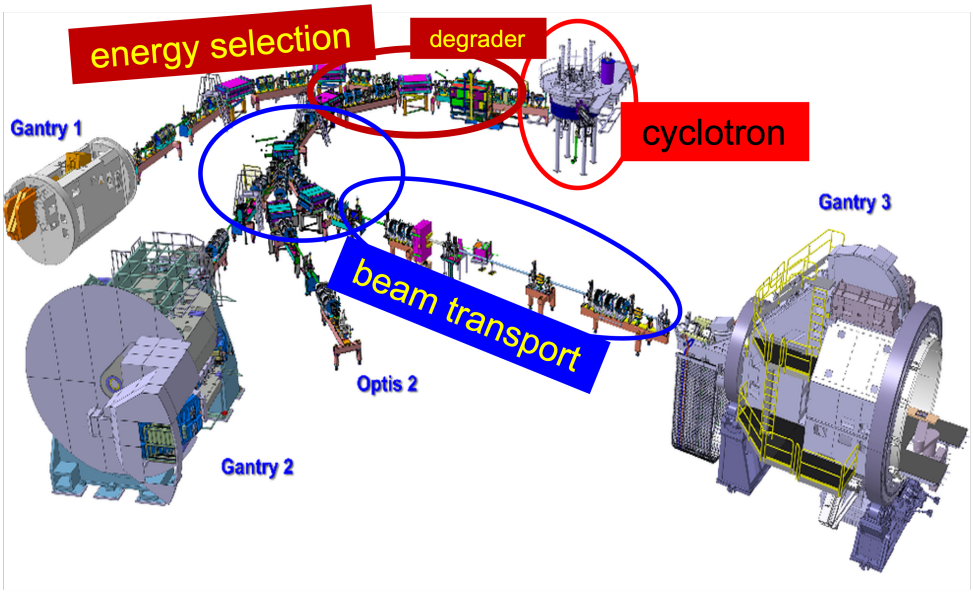

Fig. II.17.1: Overview of the PSI proton therapy facility. The protons are accelerated to 250 MeV in the cyclotron. After the degrader and energy selection, the beam is transported to one of the treatment rooms: Gantry1, 2 or 3 or the fixed beam line OPTIS2 for eye treatments.

II.17.2 Deposition of the dose in tissue

II.17.2.1 Some basic principles of radiation therapy

The goal of a radiation therapy is to kill a tumour by applying a high irradiation dose into the tumour volume. In practice, however, at the same time it is unavoidable that healthy tissue surrounding the tumour also receives a considerable radiation dose. Damage of healthy tissue is damaged, can lead to side effects and complications (sometimes very serious). Therefore, in a radiation therapy treatment the dose in and the volume of irradiated healthy tissue must be minimized to prevent or to limit these side effects. The challenge of radiotherapy is therefore to find a balance between the maximum likelihood of killing the tumour and the minimum risk of complications for the patient. This motivates the ongoing effort in radiation therapy to optimize the dose distribution.

Already shortly after the discovery of X-rays, it became clear that an appropriate dose of radiation can kill tumour cells and that the probability of killing the cells increases with the dose. However, even nowadays, with X-rays it is often a challenge to apply the necessary high radiation dose in the tumour and to sufficiently prevent irradiation of healthy tissue surrounding the tumour at the same time. By applying many techniques (accurate beam collimation, high X-ray energy from linacs, multiple irradiation directions, intensity variation within the X-ray beam, etc.), one has succeeded in reducing the dose in healthy tissue and radiation therapy has become one of the most successful treatments. However, it still happens often, that the dose in healthy tissue is limiting the dose that can be given to the tumour. Here particle therapy offers its advantage due to its beneficial distribution of the radiation dose in the patient.

In addition to sparing healthy tissue, particle therapy allows in some cases a higher dose to be applied to the tumour, which increases the chances of cure (tumour destruction), without increasing the rate of complications.

In the example shown in Fig. II.17.2, the (advanced and from seven directions) X-ray treatment of a tumour in the lung gives a dose of approx. 30% of the tumour-dose in a large volume of the surrounding tissue. This is due to the fact, that the depth-dose curve of X-rays in matter is decreasing only slowly and, depending on the X-ray energy, with typically several tens of percent with depth. The dose distribution of a proton irradiation from only three directions covers the tumour with the same way in the X-ray treatment, but the dose receiving volume of healthy tissue has been reduced dramatically. Apart from a smaller lung volume being irradiated, no dose is deposited in critical healthy tissues (heart, spinal cord).

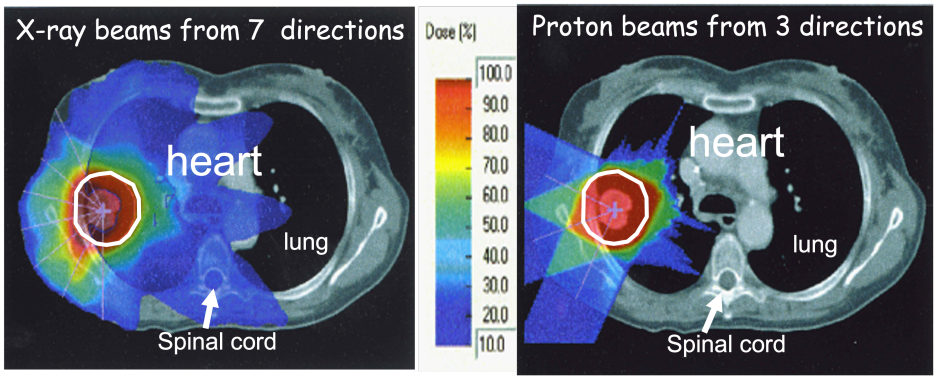

Fig. II.17.2: Comparison of dose distributions to irradiate a tumor in the lung. On the left side, it can be seen that in the X-ray irradiation from seven directions, a lot of healthy tissue (including the critical tissues heart and spinal cord) receives 30–40% of the tumor dose. The proton dose distribution from only three directions shows a very strong reduction of the irradiated healthy tissue volume, but with the same dose in the tumor. Images from Ref. [6].

II.17.2.2 Interactions of protons and ions with matter

As Wilson mentioned in 1946, this is due to the advantageous shape of the proton dose as a function of depth in the tissue and the finite, adjustable range to which the protons penetrate the tissue. In Fig. II.17.3 the proton depth-dose distributions are shown for different initial proton energies, indicating the energy dependent range, as well as the high dose deposited just before the end of the track: the so-called Bragg peak. For typically used energies, the different depth-dose curves for X-rays, protons and carbon ions are shown in Fig. II.17.4.

Since the maximum dose healthy tissue can deal with and since tissue is able to recover from a not too high dose, usually the total radiation dose (around 70 Gy) is applied in 35 daily fractions of 2 Gy. Proton treatments are applied with the same fractionation as X-ray treatments. To apply this dose of 2 Gy approximately 10^{11} protons are needed. So, to apply this dose within a minute, a proton beam current of 0.25 nA is needed at the patient. This order of magnitude of beam intensity is typical for proton therapy and cyclotrons and synchrotrons can provide these beam intensities easily.

Protons and ions crossing material will mostly lose energy by ionizing atoms (atomic number Z

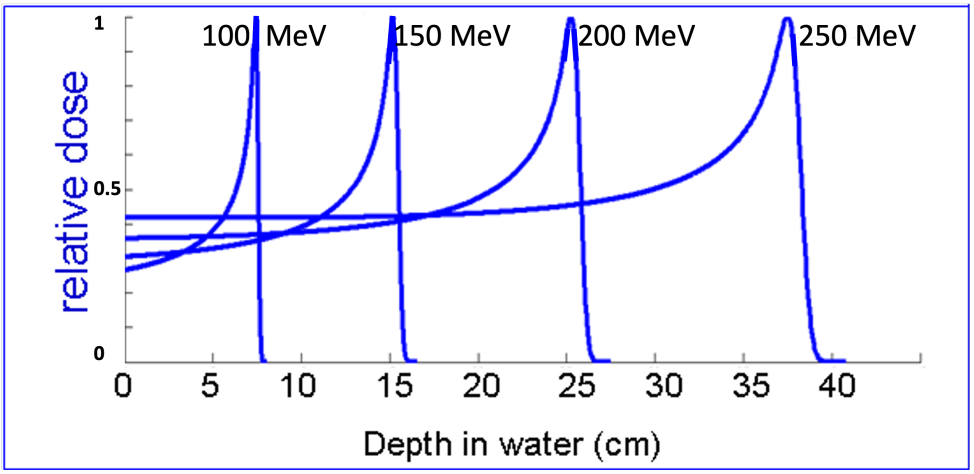

Fig. II.17.3: Depth-dose distributions of protons of different energies, showing the effect on range and on Bragg peak position.

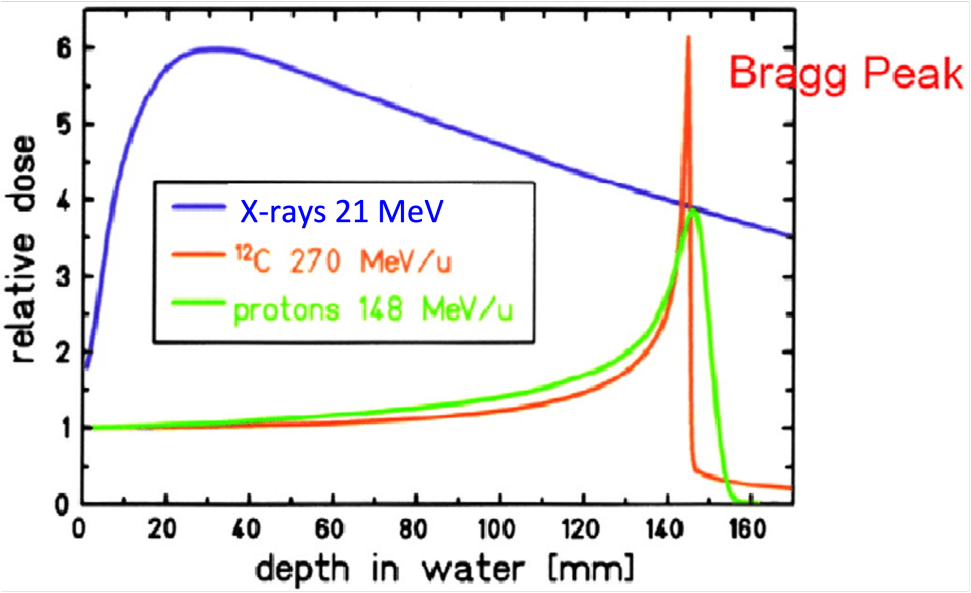

Fig. II.17.4: A comparison of the depth dose distributions for 21 MeV X rays, 270 MeV/nucl carbon ions and 148 MeV protons.

and atomic mass A) in the material with density ρ. The amount of energy lost per mass unit is in fact the locally deposited dose. This energy loss dE per covered distance dx in matter is described by the Bethe–Bloch equation, nicely explained in e.g. the text book by Leo [8]. When showing only the most relevant parameters in a simplified version of the Bethe–Bloch equation, an ion with charge z and velocity v, which crosses material with density ρ atomic number Z and atomic mass A will lose dE MeV per cm covered distance dx:

$$\frac{dE}{dx} \sim -\rho \cdot \frac{Z}{A} \cdot \frac{z^2}{v^2} \quad . \tag{II.17.1}$$

The $\frac{1}{v^2}$ causes the strong increase of the energy loss at low velocities (i.e. at low energy) occurring after slowing down, so especially just before the end of the track, where $v \rightarrow 0$. In the depth-dose distribution, this leads to the Bragg peak just before the end of the track.

For carbon ions a similar (but with a sharper Bragg peak) depth dose distribution and its advantages apply, but one should be aware of three major differences. The first difference is the smaller multiple scattering. Due to the Coulomb forces between the multiple nuclei in the material (tissue) and the proton/ion, the proton/ion is deflected from its original direction, with almost no energy loss. This multiple scattering causes a broadening of the beam after some distance. Due to the 12 times higher mass of the carbon ions, these will scatter less than the protons. In Fig. II.17.5 the width of the beam, expressed as the sigma of a Gaussian distribution, is given as a function of depth for protons and carbon ions having the same range. This gives the advantage of a beam with a sharper lateral edge than proton beams. This enables to give dose distributions with a very sharp edge, which are especially of advantage in cases where the tumour is very closely located to critical healthy tissue.

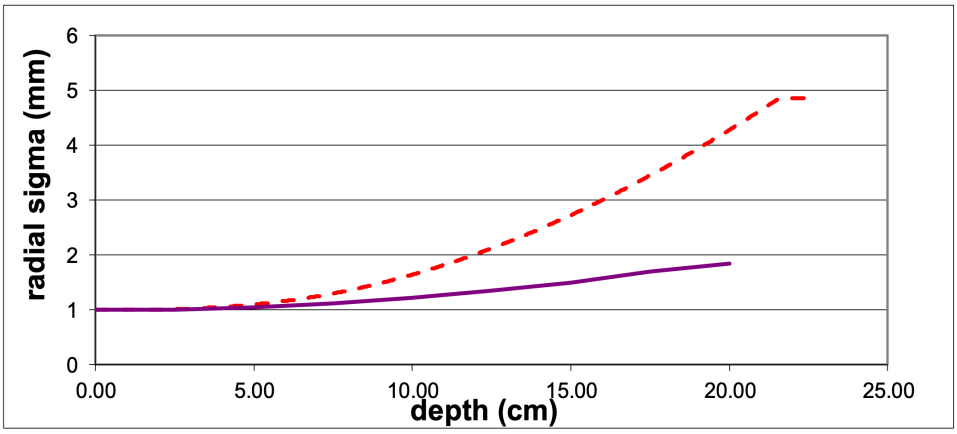

Fig. II.17.5: The width of a beam (expressed as the sigma) as a function of depth in water for carbon ions (solid line) and protons (dashed line).

The second difference is the possibility that the carbon ion breaks up into smaller ions (protons, α-particles, neutrons, etc.) due to nuclear interactions in the material crossed. Since these have a lower charge than the carbon ion and their initially high energy, their range will be larger than that of the carbon ions. As could already be seen in Fig. II.17.4, this results in a small tail, over a few cm.

The third and most important difference is the much larger energy loss along the carbon ion track. Therefore, carbon ions are so called high linear energy transfer (LET) particles. As a result, the probability to damage critical structures in a cell is much larger than for low LET radiation, like X-rays or protons, see Fig. II.17.6. Numerically the effect on cell killing is given by the radio-biological effect (RBE) [7]. The RBE value of a certain ion indicates the X-ray dose (as the reference) needed to kill a certain number of cells, relative to the dose that would be needed by the ions to achieve the same cell killing. The RBE of protons is approximately 1.1, so the same cell killing is achieved by an X-ray dose of 1.1 times the proton dose. The RBE of carbon ions can have a value in the range 1.5–5, as it depends on many parameters, such as the organ type. This RBE effect can be exploited to offer advantages in certain treatments.

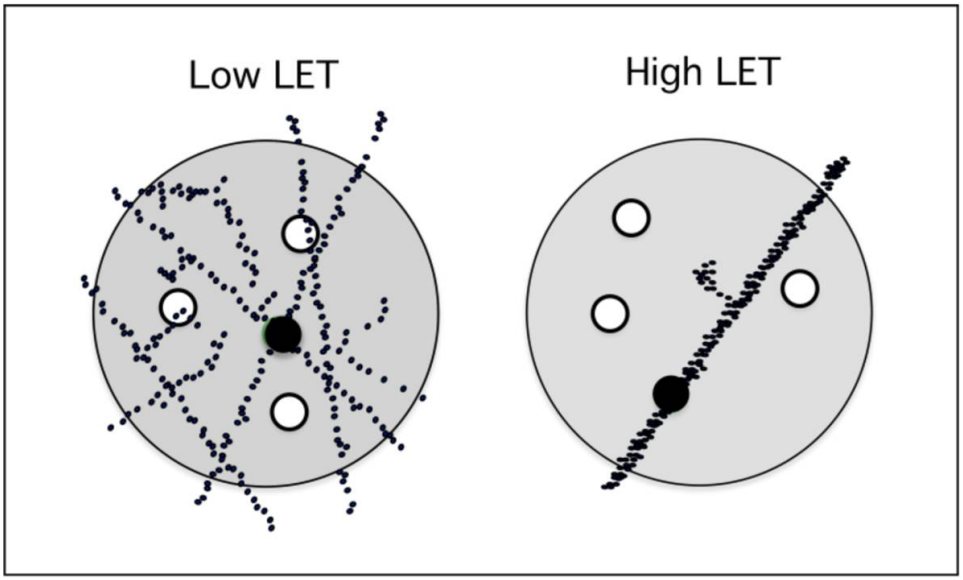

Fig. II.17.6: Schematic representation of a cell with its sensitive centers (circles), crossed by particle tracks of protons (left) and carbon ions (right). The ionization density along the carbon-ion tracks is much higher than along the proton tracks. Therefore, to damage a sensitive center in a cell (closed circle), it must be hit by several proton tracks, but only a single carbon-ion track is needed to obtain this damage [5].

II.17.2.3 Delivery of the dose

For accurate and appropriate dose delivery, the beam from a cyclotron or synchrotron is not directly applicable. Usually, the diameter of a tumour is much larger (10–100×) than the (lateral) width of the beam (typically < 1 cm, a so called pencil beam) and much thicker (5–30×) than the width of the Bragg peak. Therefore, special techniques have been developed for spreading the beam in the lateral direction as well as in depth. It is important to understand that the application of these techniques has consequences for the type of operation of the accelerator.

After aiming the beam from the desired direction by setting the gantry at the correct angle, the beam must be spread both in depth and in the lateral direction to match the volume of the tumour. Spreading in depth is done by varying the energy of the beam entering the patient. This is done by inserting an amount of low Z material (e.g. graphite) in the beam path. Behind this so-called degrader, the beam has a lower energy, depending on the amount of degrader material crossed. In Fig. II.17.7 the degrader used at PSI and its following energy selection system are shown. It consists of two multi wedges of graphite. The thickness of the material crossed by the beam is regulated by the setting the amount of insertion of the two wedges. All following magnets in the beam transport between the degrader and patient must change their fields, so that these scale with the beam momentum, coming out of the degrader. To cover a tumour with a thickness of 10 cm, approximately 20 different beam energies are needed, creating a so-called spread-out Bragg peak, as shown in the insert of Fig. II.17.7. In order to prevent long waiting times (causing long treatment times) when changing energy, this energy change is done as fast as possible. This requires an accurate (E within 0.1%) and fast (E change < 0.1 sec) system for both the degrader and all laminated magnets.

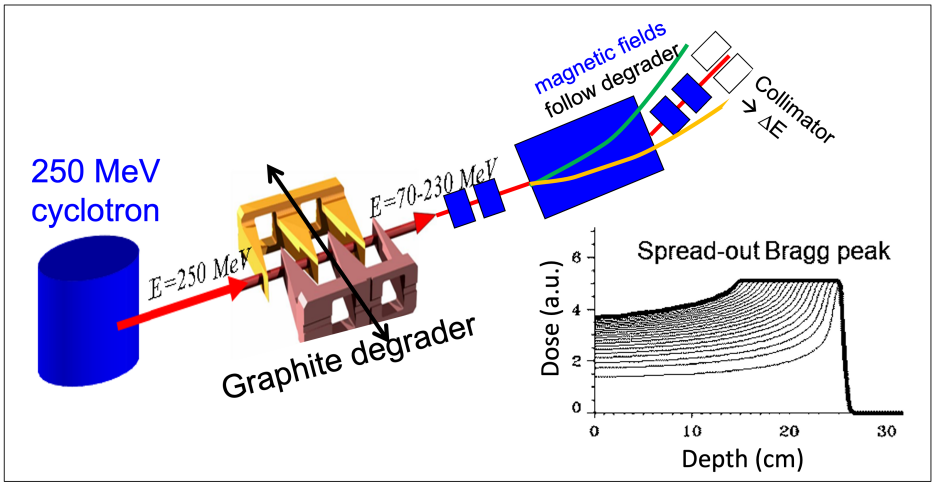

Fig. II.17.7: The 250 MeV protons from the cyclotron are degraded to an adjustable lower energy by traversing though the degrader. This is followed by a momentum (or energy) selection behind a bending magnet. In the patient's tissue the Bragg peaks created by the different energy settings are added with appropriate weight factors, to obtain a spread-out Bragg peak. The thus created dose distribution has sufficient width to cover the thickness of a tumor in depth.

In most facilities, beam spreading in the lateral direction is done by scanning the pencil beam in the lateral plane over the tumour cross section. As shown in Fig. II.17.8, this technique can be performed in a discrete way, by sequentially aiming the beam at the volume-elements in the tumour into which a dose is applied (*spot scanning*). At each volume-element, the beam is switched on until the dose for that volume element has been reached. Then the scanning magnets shift the beam direction to the next spot. A development that is in progress e.g. at PSI, is to apply *continuous scanning*. Then the beam is swept over the target volume and the dose is controlled by a variation of the beam intensity and/or the speed of the sweep, synchronous to the sweep motion. Since its clinical introduction at PSI and GSI in 1995, see Refs. [9] and [10], spot scanning is regarded as the optimal technique currently feasible in practice.

II.17.3 Accelerators currently in use for particle therapy

The maximum beam energy for proton therapy is 200–250 MeV to reach a depth of at least 25–35 cm in water (water is often used as an approximately tissue-equivalent reference material). Low energies of approximately 70 MeV are used for treatment of superficial tumours, such as melanomas in the eye. Higher energies are needed for deep lying tumours in the head or other sites in the body. For carbon ions, these ranges need a maximum energy of 400–450 MeV/nucl.

The cyclotron and the synchrotron have remained the two types of accelerators currently used in particle therapy. Several types of these machines are in use [11]. In 2022 the 13 facilities applying carbon or other ions for therapy, are using a synchrotron with a typical diameter of approx. 25 m. For protons, either synchrotrons (approx. 8 m in diameter) or cyclotrons (4.3–3.2 m diam.) are used, of which a few synchrocyclotrons (2.2–1.5 m diam). Although other types of accelerators do exist or are being developed, these are not yet suitable or routinely used for hadron therapy [13–16].

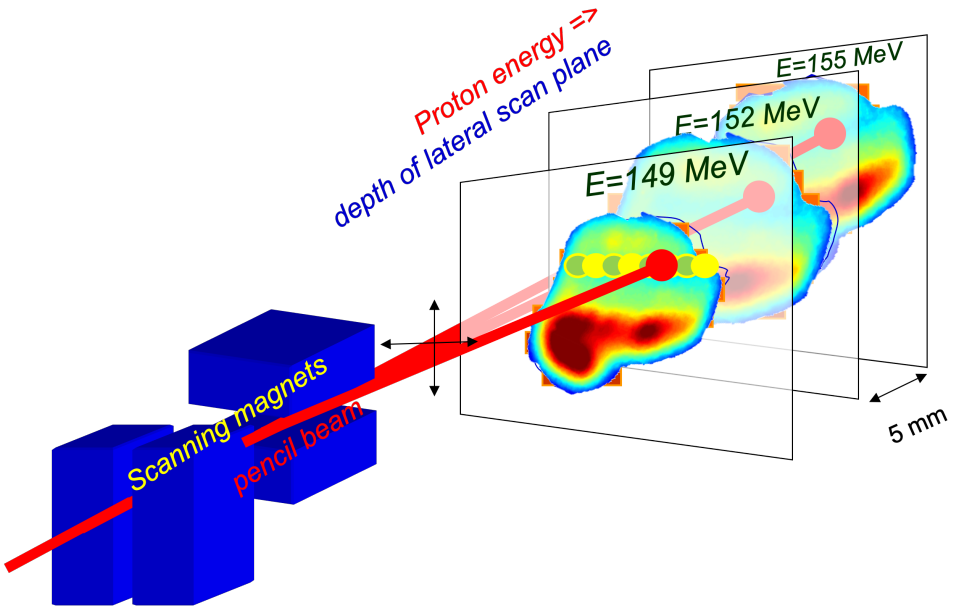

Fig. II.17.8: Protons of an energy set by the degrader and energy selection system, will have their Bragg peak at a certain depth in the patient's tissue. Here three different depths are indicated. At each depth the scanning magnets aim the beam sequentially to the spots in the lateral directions and deposit a dose that is specific for each spot.

II.17.4 The cyclotron for proton therapy at PSI

At PSI, a dedicated cyclotron is in use for proton therapy [17]. It has been in clinical operation since 2007 being the first cyclotron with superconducting coils. This has been a first step in the development towards an accelerator that has lower running costs and being as compact as possible; to reduce the investments needed to build a proton therapy facility. Superconducting coils enable the use of a stronger magnetic in the cyclotrons, reducing their radius. Due to the smaller size, the mass of these machines has reduced from 250 to 90 tons. Recent further developments have applied this technology to synchrocyclotrons [5]. These machines are even smaller and have a mass of 60–15 tons. However, due to the very large field strength, the magnetic field cannot be made homogeneous anymore. Therefore, acceleration needs to be done with a varying frequency of the RF voltage. The RF frequency varies at a rate of a few 100 to 1000 Hz. The beam from these cyclotrons is thus also pulsed with this frequency. Therefore the earlier mentioned continuous scanning is not possible with these machines.

The cyclotron at PSI (see Fig. II.17.9) has an isochronous field (2.4–3.8 T), so a CW beam is extracted (max. 800 n μA) from this cyclotron. This cyclotron uses a small proton source in the centre of the cyclotron. In this source, hydrogen gas is ionized and emitted into the cyclotron centre. Acceleration to 250 MeV is performed with 4 Dees at 100 $\mathrm{kV_{peak}}$, located in the four valleys between the hills of the cyclotron magnet poles. In the central region, the beam from the ion source is collimated, such that particles that would get lost during the acceleration process are stopped at still low energy, to prevent too much activation of the machine. To reduce beam losses at extraction, also resonant extraction is applied, in which the $\upsilon_\mathrm{r} = 1$ betatron resonance is excited in the last orbits before extraction. This increases the

orbit separation at the extractor septum. Therefore, both the beam selection in the central region and the resonant extraction help to obtain the high extraction efficiency of 60–80%. The proton source cannot react sufficiently quickly to perform the many short, but with different lengths, beam pulses for the spot scanning. Therefore a kicker magnet in the beam line at the beam output of the cyclotron is used to switch the beam on and off quickly for the spot scanning. For safety, additional possibilities to switch the beam off are implemented as well: a reduction of the accelerating RF voltage, the switching off of the ion source as well as several mechanical beam stoppers.

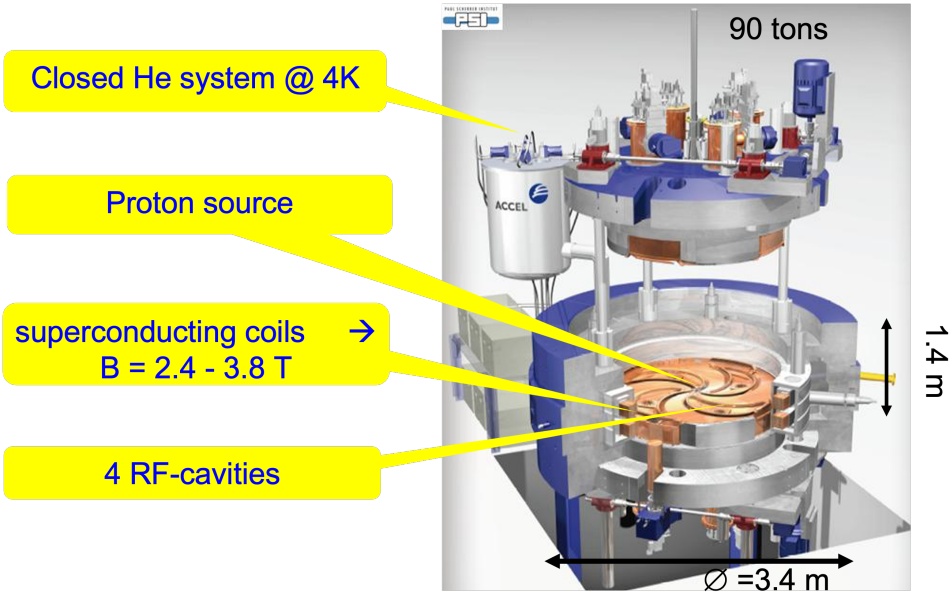

Fig. II.17.9: The 250 MeV cyclotron for proton therapy at PSI. The upper pole cap has been opened. In the artist view also the circular yoke has been cut, so that one can see the inner components: the superconducting coils in their circular cryostat and the 4 RF electrodes in the valleys between the pole hills. The SC coils are cooled with liquid helium from a cryostat on top of the cyclotron. The ion source is attached to the rod sticking out on top and located in the cyclotron center, but the source itself is too small to be visible here.

II.17.5 The proton irradiation equipment at PSI

After extraction from the cyclotron, the beam is degraded and the appropriate energy is selected (see Figs. II.17.1 and II.17.7). Then the beam is guided towards one of the treatment rooms. At PSI, the Optis2, room is used for eye treatments. Here a fixed horizontal beam is used ant the patient is sitting in a special treatment chair. The other rooms are used for irradiation of larger and more deep-seated tumours. Here a gantry is used to direct the proton beam from different directions to the tumour in a patient lying on a treatment table. This mechanical system rotates the magnets of the last part of the beam transport system around the patient. Gantries for particle therapy are of considerable size. To bend and focus the proton beam, large (and thus heavy) magnets are needed. Between the last magnet and the patient, additional space is needed for equipment, such as scanning magnets, dose monitors, etc. These 100–200 tons gantries have a typical diameter of 10–12 m.

At PSI, a compact proton gantry ("Gantry1") [9] has been optimized for pencil beam scanning. It was the first gantry in the world applying the spot scanning technique. In this gantry, a magnet is scanning the pencil beam within the bending plane of the following 90° magnet that bends the beam towards the isocentre. The beam optics of this last bending magnet has been designed such that a change of the scanning magnet strength causes a parallel shift of the pencil beam in the patient. In"Gantry2" [18] (see Fig. II.17.10) beam scanning is done with two orthogonal scanning magnets, both located before the last 90° magnet. This is similar as in Ganrtry1, so the diameter could be limited to 7.5 m. However in Gantry2 also scanning perpendicular to the bending plane is performed, so that this 90° magnet needs a relatively large gap, which makes it a very big and heavy magnet. In addition, to benefit from the fast (< 0.1 s energy steps) upstream degrader, the magnets of Gantry2 are laminated, similar as the magnets in the preceding beam transport system. Recently a third gantry has been built at PSI, see Fig. II.17.1. PSI and a commercial company, see Ref. [19], have developed this gantry in a research project. It also provides 2D lateral scanning and enables fast energy switching. Since in this gantry the scanning magnets are located behind the last bending magnet, more space is needed between the magnet and the patient, which has resulted in a gantry diameter of 10.5 m.

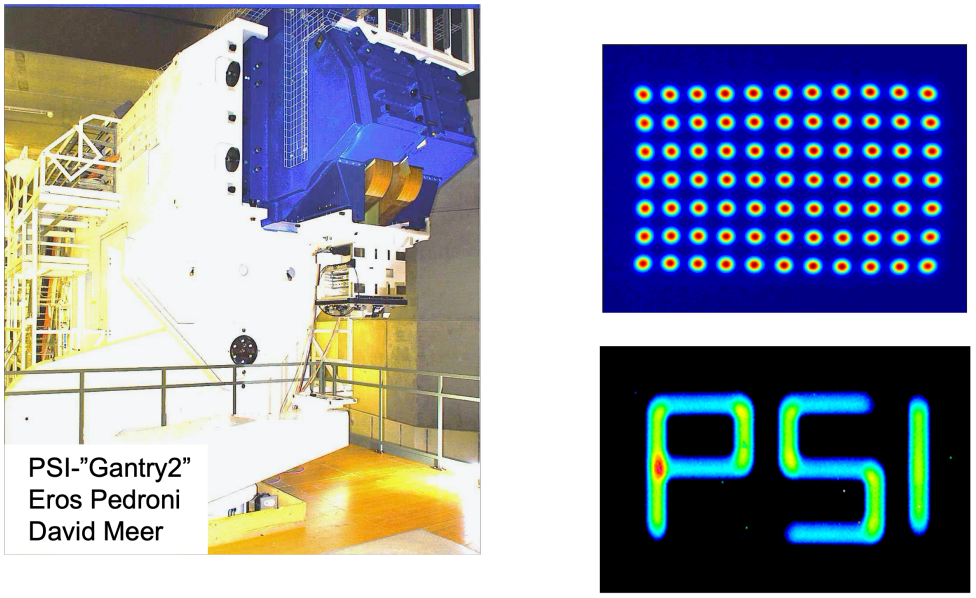

Fig. II.17.10: PSI's Gantry2 during the building phase. The big 90 degree magnet has a large aperture, so that the vertically outcoming beam is scanned both in the bending plane and in the plane perpendicular to that. A patient table can be mounted on the support before the gantry. At the beam exit side of the 90 degree magnet, equipment is mounted to measure the dose and pencil beam position during the scanning process. The scanning magnets are not visible, but mounted in the horizontal beam line just before the 90 degree magnet. On the right some lateral scanning is demonstrated.

II.17.6 Summary

Proton therapy can be applied as an irradiation therapy to treat cancer patients. The advantage of proton therapy, being one of the possible radiation therapies with ion beams, is that the radiation dose can be administered to the tumour with higher geometric accuracy when compared to the conventional irradia-

tion treatments with X-rays. In treatments with particle beams, less normal tissue is irradiated and when irradiated, most parts receive a lower dose. This reduces negative side effects of a radiation therapy and in some cases, even a higher dose can be delivered to the tumour, yielding a better curation probability but without increasing the complication probability. This better dose distribution is due to the finite range of protons or ions, when they penetrate the tissue and the high dose (Bragg peak) just before the end of the particle tracks. Especially for carbon ions, the very small effect of multiple scattering in tissue is of great advantage, since an initially sharply delimited carbon beam will remain sharply delimited with depth in tissue. To obtain sufficient penetration depth in tissue, the ions or protons are accelerated to high energies. Acceleration is done in a synchrotron or in a cyclotron. The beam from such an accelerator is transported to a treatment room. There the small pencil beam from the accelerator is scanned in 3D over the tumour volume in the patient. Fast scanning magnets perform scanning in the transverse plane and scanning in depth is performed by varying the energy of the beam. Most treatment rooms are equipped with a gantry that allows the beam of radiation to be directed in any direction toward the patient lying on a treatment couch. By irradiating from different directions, the dose to the normal tissue surrounding the tumour can be limited. Current technical developments in particle therapy aim at reducing the costs of particle therapy facilities. This should be achieved through the development of single treatment room facilities, smaller accelerators and gantries and a more efficient combination of different components. In these developments, the greatest challenge is to find a balance between reducing costs and maintaining the treatment quality achieved in the current facilities.

References

[1] R.R. Wilson, Radiological use of fast protons, *Radiology* **47** (1946) 487–491, doi:10.1148/47.5.487.

[2] J.H. Lawrence, Proton irradiation of the pituitary, *Cancer* **10** (1957) 795–798, doi:10.1002/1097-0142(195707/08)10:4<795::aid-cncr2820100426>3.0.co;2-b.

[3] Eye proton therapy: The National Centre for Eye Proton Therapy (Clatterbridge Cancer Centre, Liverpool) https://www.clatterbridgecc.nhs.uk/patients/treatment-and-support/proton-therapy, last accessed 16 June 2023.

[4] J.M. Slater *et al.*, The proton treatment center at Loma Linda University Medical Center: Rationale for and description of its development, *Int. J. Radiat. Oncol. Biol. Phys.* **22** (1992) 383–389, doi:10.1016/0360-3016(92)90058-P.

[5] Proc. CAS–CERN Accelerator School: Accelerators for Medical Applications, Vösendorf, Austria, 26 May–5 June 2015, R. Bailey (ed.), CERN Yellow Reports: School Proceedings, Vol.1/2017,CERN-2017-004-SP (CERN, Geneva, 2017), doi:10.23730/CYRSP-2017-001.

[6] T. Auberger *et al.*, Das Projekt MedAustron – Designstudie (Fotec – Forschungs- und Technologietransfer GmbH, Wr. Neustadt, 2004), ISBN: 3-200-00141-0.

[7] C.P. Karger and P. Peschke, RBE and related modeling in carbon-ion therapy, *Phys. Med. Biol.* **63** (2018) 01TR02, doi:10.1088/1361-6560/aa9102.

[8] W.R. Leo, *Techniques for nuclear and particle physics experiments*, 2nd ed. (Springer, Berlin, 1994), doi:10.1007/978-3-642-57920-2.

[9] E. Pedroni *et al.*, The 200 MeV proton therapy project at the Paul Scherrer Institute: Conceptual design and practical realization, *Med. Phys.* **22** (1995) 37–53, doi:10.1118/1.597522.

[10] T. Haberer *et al.*, Magnetic scanning system for heavy ion therapy, *Nucl. Instrum. Meth. Phys. Res. A*, **330** (1993) 296–305, doi:10.1016/0168-9002(93)91335-K.

[11] Particle Therapy Co-Operative Group (Villigen-PSI, Switzerland), https://www.ptcog.site, last accessed 16 June 2023.

[12] Particle therapy facilities in clinical operation (Particle Therapy Co-Operative Group, Villigen-PSI, Switzerland) https://www.ptcog.site/index.php/facilities-in-operation-public, last accessed 16 June 2023.

[13] J.M. Schippers, Beam delivery systems for particle radiation therapy: Current status and recent developments, *Rev. Accel. Sci. Tech.* **2** (2009) 179–200, doi:10.1142/9789814299350_0009.

[14] C.-M.C. Ma and T. Lomax, *Proton and carbon ion therapy* (CRC Press, Boca Raton, FL, USA, 2013), 10.1201/b13070.

[15] H. Paganetti, *Proton therapy physics*, 2nd ed. (CRC Press, Boca Raton, FL, USA, 2018), doi:10.1201/b22053.

[16] J.M. Schippers and A. Lomax, Emerging technologies in proton therapy, *Acta Oncol.* **50** (2011) 838–850, 10.3109/0284186X.2011.582513.

[17] J.M. Schippers *et al.*, The SC 250 MeV cyclotron and beam lines of PSI's new protontherapy facility PROSCAN, *Nucl. Instr. Meth. B* **261** (2007) 773–776, doi:10.1016/j.nimb.2007.04.052

[18] E. Pedroni *et al.*, The PSI Gantry 2: A second generation proton scanning gantry, *Z. Med. Phys.* **14** (2004) 25–34, doi:10.1078/0939-3889-00194.

[19] A. Koschik *et al.*, PSI GANTRY 3: Integration of a new gantry into an existing proton therapy facility, Proc. IPAC2016, Busan, Korea, pp. 1927–1929, doi:10.18429/JACoW-IPAC2016-TUPOY014.